

For improvements in chromatic scales and luminescent fluxes of white lights: developing a dual-layer remote phosphor structure

Van Liem Bui¹, Nguyen Thi Phuong Loan², Hai Minh Nguyen Tran³

¹Faculty of Fundamental Science, Industrial University of Ho Chi Minh City, Ho Chi Minh City, Vietnam

²Faculty of Fundamental, Posts and Telecommunications Institute of Technology, Ho Chi Minh City, Vietnam

³Faculty of Mechanical - Electrical and Computer Engineering, School of Engineering and Technology, Van Lang University, Ho Chi Minh City, Vietnam

Article Info

Article history:

Received Jun 18, 2021

Revised Nov 13, 2022

Accepted Nov 23, 2022

Keywords:

Color rendering index

Dual-layer phosphor

Luminous flux

Mie-scattering theory

WLEDs

ABSTRACT

This study compares red-phosphor LaOF:Eu³⁺ impacts on a single-film remote phosphor configuration (SRPC) and a double-film remote phosphor configuration (DRPC). Mie theory is used to demonstrate the relationship between light flux and color quality. SRPC is a phosphor layer consisting of LaOF:Eu³⁺ particles mixed with YAG:Ce³⁺. Meanwhile, DRPC is two separate films of red and yellow phosphors. To increase scattering properties, we added 5% SiO₂ into phosphor layers. The differences in structure affect significantly white light emitting diodes' (WLEDs') optical properties. Attained figures and statistics show that the color rendering indices (CRIs) increase along with the concentrations of both structures, and these numbers are approximately similar. However, DRPC exhibits a color quality scale (CQS) of 74 in all examined chromatic temperatures (5600 K – 8500 K), which is greater than SRPC's 71 at 8500 K. Besides, the luminous efficiencies (LEs) in DRPC are more outstanding than that of SRPC, at given LaOF:Eu³⁺ concentration percentages (2%–14%). To summarize, DRPC offers greater benefits in luminous flux and color quality, compared to SRPC. Choosing the proper red light phosphor concentration, on the other hand, becomes a crucial aspect of achieving the ideal CQS and LEs.

This is an open access article under the [CC BY-SA](https://creativecommons.org/licenses/by-sa/4.0/) license.



Corresponding Author:

Hai Minh Nguyen Tran

Faculty of Mechanical - Electrical and Computer Engineering, School of Engineering and Technology

Van Lang University, Ho Chi Minh City, Vietnam

Email: minh.nth@vlu.edu.vn

1. INTRODUCTION

A circadian light source with tunable color temperature can benefit human life quality. Having bright and calming color light in the workplace in the daytime can also improve productivity [1]-[3]. Using dim, red-rich incandescent lighting when the moon rises may also help you feel more relaxed and tranquil. In that case, humans get used to circadian sources during evolution. It would be appropriate to use white light emitting diodes (LEDs), or white light emitting diodes (WLEDs), that emulate the daylight color temperatures (CTs) from the sun for daytime activities, while it is ideal for LEDs with lower CTs to be used at daybreak and nighttime. The difficulty in designing the desired cluster of the white LED for the mentioned prospects is to attain high color rendering indices (CRIs) over a wide variety of CTs while maximizing their luminous efficiencies (LEs) [4]-[6]. There are some profound analyses showing WLEDs setups that present remarkably adjustable correlated chromatic temperatures (CCTs) [7], [8]. The outcome shows that one of the easiest approaches to high LE and color rendering indices (CRI), especially the R9CRI for the bright red emission, is to formulate a phosphor-covered/red/blue LED (PC/R/B LED) model. Specifically, this LED model

comprises a phosphor-covered LED (PC LED), in which the green and orange phosphors are applied and stimulated by the blue chip, a red LED, and a blue LED [9]-[12]. The CCT-adjustable PC/R/B LED setup exhibited CRI and R9 values ranging from 90 to 96, along with LEs varying from 105 to 119 lm/W, when the CCT range is from 2722 K to 6464 K. On the other hand, this combined CCT-adjustable LED model cannot provide CCT white light having both CRI and R9 above 96 [13]-[15]. Apart from the down-conversion energy loss of phosphors, until now, no one has investigated the photometric optimization of the CCT-adjustable WLED using remote phosphor configurations (RPCs) with high CRI. Hence, an urge to demonstrate a photometric optimization model for a CCT-changeable WLED model, which accesses the down-conversion energy loss, with a great level of CRIs has emerged in the research field [16]-[18]. By satisfying the criteria at CCTs 2700 K to 6500 K, both CRI and R9 over 98, with differences in color shades below 0.0054, assessed from the Planckian or daylight locus on the CIE 1960 UV chromatic diagram (Duv). To obtain a desired CCT-adjustable red/yellow/conversion (R/Y/C) white-emission LED setup, the component LEDs used for designing are the PC LED types. In detail, they are AlGaInP-based PC LEDs with direct red-emission, PC LEDs with yellow-emission that consist of green-emitting and orange-emitting silicate phosphors, and cyan-emission PC LEDs with silicate green phosphors. All of them are excited by an InGaN blue chip. PiG not only improves the LE and heat consistency of WLEDs, but it also provides color quality benefits that are only mentioned or demonstrated in a few kinds of research. In this study, the novel RPC designed with two separate phosphor films, called double-film remote phosphor configuration (DRPC), is presented to access the improvement of optical properties, especially, the LE and chroma feature of WLEDs. Furthermore, using Mie scattering theory, the optical properties of two RPC types, including the single-film RPC (SRPC) and DRPC, are convincingly demonstrated.

2. DETAIL OF EXPERIMENT AND SIMULATION

As shown in Figure 1(a), WLEDs, with average CCTs of 8500 K, 7700 K, 7000 K, 6600 K, and 5600 K and built with RPCs, are created with the commercial software LightTools 9.0 [19]. Additionally, the simulating process by LightTools employs a Monte Carlo ray-tracing technique. Figure 1(b) shows the physical model of WLEDs in 3D simulation, which is then used for lighting simulations of distant packages. As shown in Figure 1(c), SRPC is performed with a phosphorous layer composed of LaOF:Eu³⁺ and a yttrium aluminum garnet (YAG) combination. DRPC, on the other hand, is made up of two distinct red and yellow phosphor layers, as seen in Figure 1(d). The bottom length of the mirror in this physical form of WLEDs is 8 mm, along with a 2.07 mm height and a 9.85 mm length for the top surface. A fixed thickness of 0.08 mm remote phosphor coating is applied to the 9 LED chips. As in Figure 1(b), the cavity of the reflector confines 3 parallel columns of LED chips whose square base is 1.14 mm and height is 0.15 mm. At a wavelength of 455 nm, each blue chip emits 1.16 W of radiant flux. The concentration of LaOF:Eu³⁺ phosphor particle changes from 2% to 30% while the weight percentage of SiO₂ particles in phosphor compounding is constant at 5%. Additionally, the percentage of YAG:Ce³⁺ amount is regulated for maintaining average CCT values.

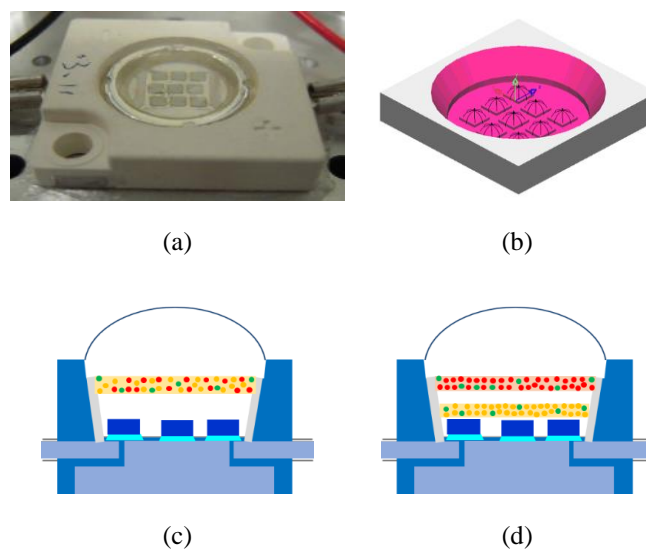


Figure 1. Illustration of the modeled WLEDs: (a) Physical model of a WLED; (b) The LightTools-simulated WLED cluster; (c) SRPC with SiO₂ (green) and LaOF:Eu³⁺ (red) in YAG:Ce³⁺ layer (yellow); and (d) DRPC with SiO₂ in LaOF:Eu³⁺ layer and YAG:Ce³⁺ layer

The optical properties of SiO₂ and LaOF:Eu³⁺ phosphor particles can be created using the LightTools 9.0 program [20]-[22]. The diffuses, such as SiO₂ and LaOF:Eu³⁺ phosphor, have optional refractive indexes (RIs) of 1.54 and 1.80. In the Mie simulation, the SiO₂ particles are considered orbicular with an average radius of 3 μm. The phosphor particles have a 7.25 μm average radius and a 1.83 RI, and the silicone glues' RI is 1.5, at all wavelengths. The diffusional particle density is distinguished to set the average CCT value. When the weight percentage of diffuses grows, the weight of YAG:Ce³⁺ phosphor must decrease to maintain the average CCT value.

LaOF:Eu³⁺ phosphors are synthesized using the sol gel technique. The critical chemical components for the LaOF:Eu³⁺ synthesis are lanthanum oxide, europium oxide, and lanthanum trifluoride, which are detailed in Table 1, respectively. The initial slurry is formed by dissolving the three components in methanol. This slurry then gets a more solid form by drying in the air and following powdered. The powder is burned in capped quartz tubes loaded with N₂ and lasts an hour. The burning process is carried out 2 times at 1000 °C and 1200 °C, respectively, each of which is accompanied by a powdering process. The collected LaOF:Eu³⁺ exhibits red emission and peak emissions of 1.981–2.145 eV within the 580–600 nm wavelength band.

Table 1. Composition of red-emitting LaOF:Eu³⁺ phosphor

Ingredient	Mole %	By weight (g)
La ₂ O ₃	61 (of La)	99.4
Eu ₂ O ₃	5 (of Eu)	8.8
LaF ₃	34	66.6

3. SCATTERING COMPUTATION

Expressions (1) and (2) can be used to compute anisotropy scattering $g(\lambda)$ and scattering coefficient $\mu_{sca}(\lambda)$ using Mie-scattering theory [23]-[26].

$$g(\lambda) = 2\pi \int_{-1}^1 p(\theta, \lambda, r) f(r) \cos \theta d \cos \theta dr \quad (1)$$

$$\mu_{sca}(\lambda) = \int N(r) C_{sca}(\lambda, r) dr \quad (2)$$

In the equation of anisotropy scattering, $p(\theta, \lambda, r)$ indicates the phase function, with λ – the wavelength (nm), r – the diffusing particles' radius (μm), and θ – the scattering angle (°C), while $f(r)$ indicates the size distribution function of the diffusing particles in the phosphorous layer. For the scattering coefficient formula, $N(r)$ stipulates the distribution density of the diffusing particles (mm³), and C_{sca} indicates the scattering cross-sections (mm²). $N(r)$ and $f(r)$ calculations are expressed as:

$$f(r) = f_{dp}(r) + f_{pp}(r) \quad (3)$$

$$N(r) = N_{dp}(r) + N_{pp}(r) \quad (4)$$

Accordingly, $N(r)$ comprises $N_{dp}(r)$ – distribution density of diffusing particles and $N_{pp}(r)$ – distribution density of phosphors that are the yellow YAG:Ce³⁺ in this study. $f_{dp}(r)$ and $f_{pp}(r)$ are the size distribution functions of the diffusing and phosphor particles, respectively. Meanwhile, with Mie-scattering basis, C_{sca} is determined with the (5).

$$C_{sca} = \frac{2\pi}{k^2} \sum_0^\infty (2n - 1) (|a_n|^2 + |b_n|^2) \quad (5)$$

Where $k = 2\pi/\lambda$, while a_n and b_n are collected using (6) and (7).

$$a_n(x, m) = \frac{\psi'_n(mx)\psi_n(x) - m\psi_n(mx)\psi'_n(x)}{\psi'_n(mx)\xi_n(x) - m\psi_n(mx)\xi'_n(x)} \quad (6)$$

$$b_n(x, m) = \frac{\psi'_n(mx)\psi_n(x) - \psi_n(mx)\psi'_n(x)}{\psi'_n(mx)\xi_n(x) - \psi_n(mx)\xi'_n(x)} \quad (7)$$

Where $x = k \cdot r$, m is the refractive index, and $\psi_n(x)$ and $\xi_n(x)$ are the Riccati–Bessel function.

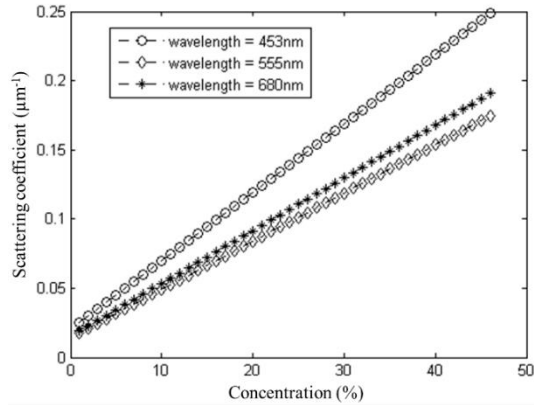


Figure 2. Scattering coefficients of LaOF:Eu³⁺ in proportion to wavelengths of 453 nm, 555 nm, and 680 nm

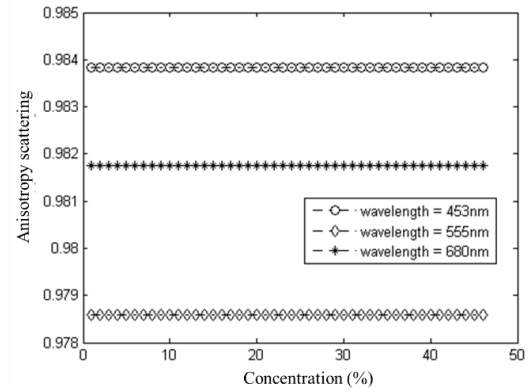


Figure 3. Anisotropy scattering of LaOF:Eu³⁺ in proportion to wavelengths of 453 nm, 555 nm, and 680 nm

The scattering coefficients increase with the concentration of LaOF:Eu³⁺ phosphor, as seen in Figure 2. The scattering effects of LaOF:Eu³⁺, and SiO₂ particles have a significant impact on RPC-WLEDs. The phosphor LaOF:Eu³⁺ has a better absorption capacity than LED blue light. As a result, in RPC-WLEDs, the dominance of output red-light can be employed to compensate for red-light. Furthermore, increasing the absorption ability of pc-LEDs by 5% wt. SiO₂ concentration used to enhance scattering events also boosts. Additionally, improving the absorption capacity of pc-LEDs by 5% wt. SiO₂ concentrations used to promote scattering events also improve pc-LED absorption. As a result, LaOF:Eu³⁺, and SiO₂ particles are a part of these RPC-WLEDs' production higher performance in re-generating light chroma. Figure 3 shows the anisotropy factor of LaOF:Eu³⁺ particles at wavelengths of 453 nm, 555 nm, and 680 nm, revealing that the 680 nm anisotropy factor is larger than the 555 nm anisotropy factor. Furthermore, when compared to other wavelengths, 453 nm has the highest anisotropy factor values. In other words, LaOF:Eu³⁺ particles help RPC-WLEDs maintain color consistency.

Besides, the impact of the LaOF:Eu³⁺ on color features of the white light is also demonstrated via the reduced scattering coefficients (RSCs) and angular scattering amplitudes (ASAs). The RSCs can be expressed by the relation between the scattering coefficient and the anisotropy scattering, as in the following equation, in which the RSC is indicated by δ_{sca} .

$$\delta_{sca} = \mu_{sca}(1 - g) \quad (8)$$

Besides, the ASAs can be acquired from the phase function $p(\theta, \lambda, r)$ that is demonstrated by (9).

$$p(\theta, \lambda, r) = \frac{4\pi\beta(\theta, \lambda, r)}{k^2 c_{sca}(\lambda, r)} \quad (9)$$

The ASAs in the formulas are symbolized by $\beta(\theta, \lambda, r)$, $S_1(\theta)$ and $S_2(\theta)$, which are calculated:

$$\beta(\theta, \lambda, r) = \frac{1}{2} [|S_1(\theta)|^2 + |S_2(\theta)|^2] \quad (10)$$

$$S_1 = \sum_{n=1}^{\infty} \frac{2n+1}{n(n+1)} [a_n(x, m)\pi_n(\cos \theta) + b_n(x, m)\tau_n(\cos \theta)] \quad (11)$$

$$S_2 = \sum_{n=1}^{\infty} \frac{2n+1}{n(n+1)} [a_n(x, m)\tau_n(\cos \theta) + b_n(x, m)\pi_n(\cos \theta)] \quad (12)$$

The calculated RSCs and ASAs are displayed in Figure 4 and Figure 5, respectively. As depicted in both figures, the scattering of the blue light is greatly influenced. The RSCs (Figure 4) in three different wavelengths of blue (453 nm), green (555 nm), and red (680 nm) increase with the concentration of LaOF:Eu³⁺. However, the difference among these wavelengths is negligible. The angular light scattering within the blue wavelength is more significant than in the other wavelengths (Figure 5). This once emphasizes the improved blue light scattering as a function of LaOF:Eu³⁺ addition. Moreover, the scattering in the other light wavelength is boosted, significantly contributing to leveling up the general chromaticity of the white lights.

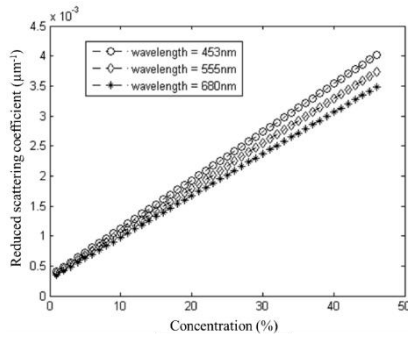


Figure 4. LaOF:Eu³⁺ reduced scattering coefficients in wavelengths of 453 nm, 555 nm, and 680 nm

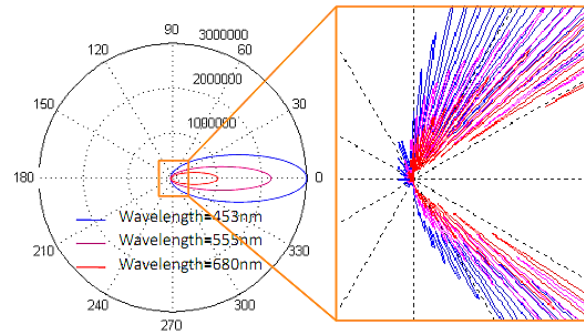


Figure 5. LaOF:Eu³⁺ angular scattering amplitudes in wavelengths of 453 nm, 555 nm, and 680 nm

4. RESULTS AND CONCLUSION

According to Figure 4, LaOF:Eu³⁺ displays lower scattering coefficients as the wavelength value increase (453 nm > 555 nm > 680 nm). The color quality of RP-WLEDs is profited by the scattering stability of LaOF:Eu³⁺. Then, using the MATLAB tool to calculate the angular scattering amplitudes of LaOF:Eu³⁺. According to the findings in Figure 5, LaOF:Eu³⁺ particles have a significant advantage in blue-light scattering. We need to increase the amount of blue light emitted to reduce the yellow ring phenomena. Similarly, LaOF:Eu³⁺ granules are applied for not only red energy enhancement but also efficient blue light production and distribution. These computations' results significantly contribute to the demonstration of findings in Figure 6, Figure 7, and Figure 8.

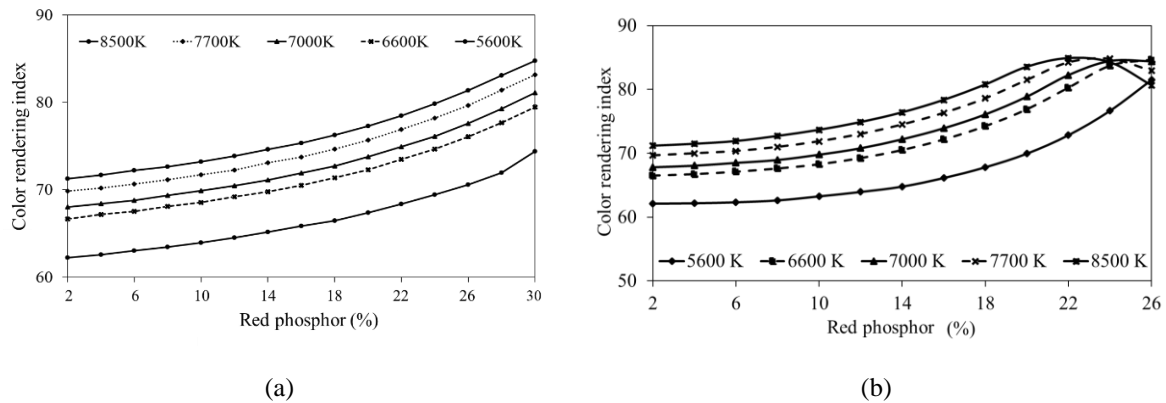


Figure 6. CRI factors with different LaOF:Eu³⁺ concentrations in (a) SRPC and (b) DRPC

The divergence in CRI value between two structures SRPC (Figure 6(a)) and DRPC (Figure 6(b)) is not significant. Both SRPC and DRPC present the increasing CRI following the increasing weight percentage of LaOF:Eu³⁺. Furthermore, these RPCs have their CRIs direct proportional to the CCT values, and thus, achieve the highest CRI of ~85 at 8500 K, with the LaOF:Eu³⁺ concentration ranging from 2 to 22 wt%. This is the vital notes on the CRI improvement for SRPC and DRPC. The challenges in controlling CRI at the high average CCTs (8500 K) are an outstanding problem, but phosphor LaOF:Eu³⁺ has offer a potential solution to this. The next color evaluating parameter is CQS which carefully considers three chroma-related factors: CRI, desirable color performance in observer's visuality, and color coordinates. Thus, it can be implied that CRI is merely one of the color quality evaluation indices, and CQS becomes an advanced and critical index to evaluate color quality. When the concentration of LaOF:Eu³⁺ surpasses 22 wt%, SRPC has its CRI continued growing. In the meantime, DRPC's CRI appears to be decreasing in all ACCTs. The CQS factor shows the same tendency in both structures, which depicted in Figure 7. In SRPC structure, CQS reaches its peak at the CCT of 7700 K is 71, see Figure 7(a). While in Figure 7(b), the structure of DRPC exhibits CQS value of 74 in nearly all ACCTs. Therefore, DRPC brings better color quality than SRPC.

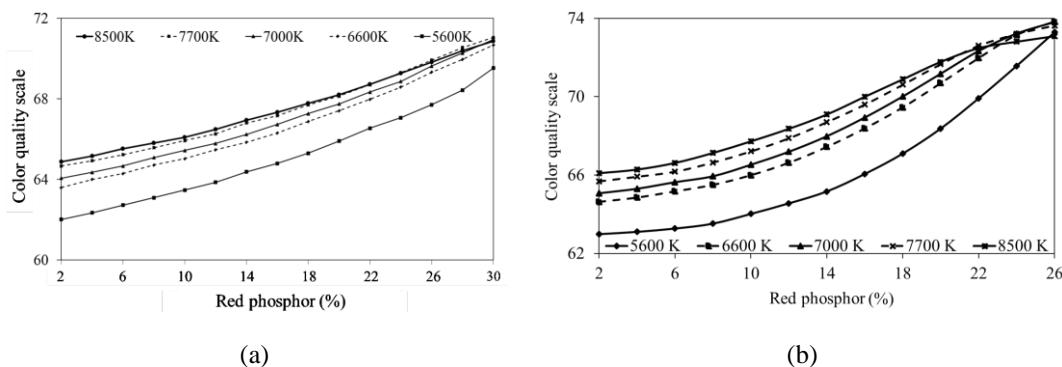


Figure 7. CQS factors with different LaOF:Eu^{3+} concentrations in (a) SRPC and (b) DRPC

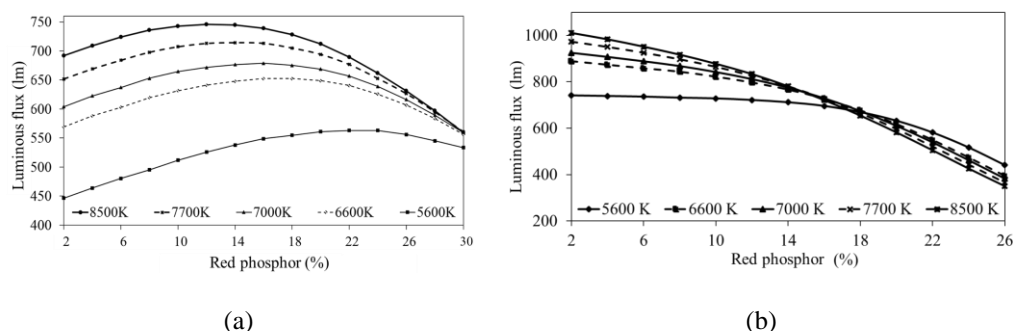


Figure 8. LEs with different LaOF:Eu^{3+} concentrations in (a) SRPC and (b) DRPC

Furthermore, with the demonstration of ASAs Figure 5 that the number of angular scattering amplitudes of LaOF:Eu^{3+} at 453 nm is the largest compared to those at 555 nm or 680 nm, increasing the LaOF:Eu^{3+} content improves blue light scattering significantly. This interest is not just for boosting color quality but also for increasing luminous flux. However, if the LaOF:Eu^{3+} concentration exceeds 14% in SRPC, significant backscattering occurs, resulting in a drop in luminous flux. In certain circumstances, the light output steadily decreases after attaining its maximum intensity, as seen in Figure 8(a). Figure 8(b) presents a vital shrinkage in LE of DRPC with the increasing red-emitting LaOF:Eu^{3+} phosphor concentration. It is because the light transmission energy decreases significantly after passing through the LaOF:Eu^{3+} sheet. With 2%–14% LaOF:Eu^{3+} , nevertheless, the luminous flux of DRPC is consistently more intense than that of SRPC in all ACCTs. Accordingly, besides CQS, the DRPC structure yields higher brightness for WLEDs than SRPC.

5. CONCLUSION

This research focuses on two issues and proposes some solutions. First of all, it is the comparison of CQS and LED between SRPC and DRPC structures. The second is to analyze red-phosphor LaOF:Eu^{3+} influences on the CQS, CRI, and LE of these above structures. To achieve the expected CQS and LE, both factors of PC WLED internal structure and concentration must be decided at the same time. The outcome displayed that CRI and CQS increase with the growing concentration of phosphor LaOF:Eu^{3+} . When employing DRPC at ACCTs of 5600 K–8500 K, CQS can approach 74, but luminous flux (LF) drops dramatically. Even though, LE of DRPC is always vastly higher than SRPC at all ACCTs of 2%–14% LaOF:Eu^{3+} . The scattering features of LaOF:Eu^{3+} , such as the scattering coefficients – $\mu_{sca}(\lambda)$, anisotropy factor – $g(\lambda)$, the RSC – $\delta_{sca}(\lambda)$, and the ASA – $S_1(\theta)$ and $S_2(\theta)$, may explain this result. To sum up, while the CRIs of SRPC and DRPC are relatively equal, either CQS or LE of DRPC is superior to SRPC's figures. Besides, the concentrations of LaOF:Eu^{3+} are recommended to be kept within an appropriate range to achieve the ideal CQS accompanied by stable and strong LEs.




ACKNOWLEDGEMENTS

This study was financially supported by Van Lang University, Vietnam.




REFERENCES

- [1] Y. H. Kim, N. S. M. Viswanath, S. Unithrattil, H. J. Kim, and W. B. Im, "Review—Phosphor Plates for High-Power LED Applications: Challenges and Opportunities toward Perfect Lighting," *ECS Journal of Solid State Science and Technology*, vol. 7, no. 1, 2018, doi: 10.1149/2.0181801jss.
- [2] J. L. Leañó Jr., M. -H. Fang, and R. -S. Liu, "Review—Narrow-Band Emission of Nitride Phosphors for Light-Emitting Diodes: Perspectives and Opportunities," *ECS Journal of Solid State Science and Technology*, vol. 7, no. 1, 2018, doi: 10.1149/2.0161801jss.
- [3] T. Jansen, J. Gorobez, and T. Jüstel, "Communication—Optical Properties of Red Emitting HK3SnF8:Mn4+ as a Color Converter for Next Generation Warm White LEDs," *ECS Journal of Solid State Science and Technology*, vol. 7, no. 6, 2018, doi: 10.1149/2.0311806jss.
- [4] A. K. Dubey, M. Gupta, V. Kumar, V. Singh, and D. S. Mehta, "Blue laser diode-pumped Ce:YAG phosphor-coated cylindrical rod-based extended white light source with uniform illumination," *Laser Physics*, vol. 29, no. 5, 2019, doi: 10.1088/1555-6611/ab05c0.
- [5] J. S. Li, Y. Tang, Z. -T. Li, K. Cao, C. -M. Yan, and X. -R. Ding, "Full spectral optical modeling of quantum-dot-converted elements for light-emitting diodes considering reabsorption and reemission effect," *Nanotechnology*, vol. 29, no. 29, 2018, doi: 10.1088/1361-6528/aac1b0.
- [6] S. Li, R. -J. Xie, T. Takeda, and N. Hirosaki, "Critical Review—Narrow-Band Nitride Phosphors for Wide Color-Gamut White LED Backlighting," *ECS Journal of Solid State Science and Technology*, vol. 7, no. 1, 2018, doi: 10.1149/2.0051801jss.
- [7] K. K. Gupta, S. Som, and C. -H. Lu, "Synthesis and luminescence characterization of Ce3+ activated Y2CaAl2MgZr2O12 garnet phosphor for white light emitting diodes," *Materials Research Express*, vol. 6, no. 12, 2020, doi: 10.1088/2053-1591/ab62eb.
- [8] D. Kundaliya, N. V. Malm, and K. C. Mishra, "Integration of YAG:Ce Thin Film Wavelength Converter on III-V Blue LED via a Laser Lift-Off Process," *ECS Journal of Solid State Science and Technology*, vol. 7, no. 1, 2018, doi: 10.1149/2.0111801jss.
- [9] S. Adachi, "Review—Mn4+-Activated Red and Deep Red-Emitting Phosphors," *ECS Journal of Solid State Science and Technology*, vol. 9, no. 1, 2020, doi: 10.1149/2.0022001JSS.
- [10] S. K. Sharma, T. Tingberg, I. Carrasco, M. Bettinelli, D. Kuylenstierna, and M. Karlsson, "Photoluminescence Properties and Fabrication of Red-Emitting LEDs based on Ca9Eu(VO4)7 Phosphor," *ECS Journal of Solid State Science and Technology*, vol. 9, no. 1, 2020, doi: 10.1149/2.0052001JSS.
- [11] N. S. Zailani, M. F. Ghazli, R. Hussin, S. Z. A. Rahim, and M. N. M. Saad, "Synthesis and Luminescent Properties of LiEu(0.50-x)Gd0.50 (WO4)2Smx Red Phosphor," *IOP Conference Series: Materials Science and Engineering*, 2018, vol. 374, doi: 10.1088/1757-899X/374/1/012026.
- [12] Q. Wei, Z. Yang, Y. Liu, Q. Zhou, and Z. Wang, "Communication—Highly Efficient Red-Emitting Phosphor Na2SiF6:Mn4+ Prepared in H3PO4 Environment," *ECS Journal of Solid State Science and Technology*, vol. 9, no. 2, 2020 doi: 10.1149/2162-8777/ab709b.
- [13] D. Shi *et al.*, "Communication—Luminescence Properties of a Novel 1 Rb2KGaF6:Mn4+ Red-Emitting Phosphor for Solid-State Lighting," *ECS Journal of Solid State Science and Technology*, vol. 9, no. 12, 2020, doi: 10.1149/2162-8777/abc835.
- [14] N. Dhananjaya, S. R. Yashodha, and C. Shivakumara, "The orange red luminescence and conductivity response of Eu3+ doped GdOF phosphor: synthesis, characterization and their Judd-Ofelt analysis," *Materials Research Express*, vol. 6, no. 12, 2019, doi: 10.1088/2053-1591/ab4a6b.
- [15] Y. Masubuchi *et al.*, "Large red-shift of luminescence from BaCN2:Eu2+ red phosphor under high pressure," *Applied Physics Express*, vol. 13, no. 4, 2020, doi: 10.35848/1882-0786/ab8055.
- [16] T. G. Lim, Y. N. Ahn, H. W. Park, and J. S. Yoo, "Red-Shifted Absorption of a Mn4+-Doped Germanate Phosphor by Crystal Distortion," *ECS Journal of Solid State Science and Technology*, vol. 7, no. 1, 2017, doi: 10.1149/2.0241801jss.
- [17] R. Kobayashi, H. Tamura, Y. Kamada, M. Kakihana, and Y. Matsushima, "A New Host Compound of Aluminum Lithium Fluoride Oxide for Deep Red Phosphors Based on Mn4+, Fe3+, and Cr3+," *ECS Transactions*, vol. 88, no. 1, 2019, doi: 10.1149/08801.0225ecst.
- [18] S. Sakurai, T. Nakamura, and S. Adachi, "Synthesis and properties of Rb2GeF6:Mn4+ red-emitting phosphors," *Japanese Journal of Applied Physics*, vol. 57, no. 2, 2018, doi: 10.7567/JJAP.57.022601.
- [19] Y. Wen, Z. Li, D. Chen, and S. Man, "Preparation and Optical Properties of Cr3+ Doped CaAlBO4 Red Phosphor," *IOP Conference Series: Earth and Environmental Science*, vol. 714, 2021, doi: 10.1088/1755-1315/714/3/032087.
- [20] T. Jansen *et al.*, "Narrow Band Deep Red Photoluminescence of Y2Mg3Ge3O12:Mn4+,Li+ Inverse Garnet for High Power Phosphor Converted LEDs", *ECS Journal of Solid State Science and Technology*, vol. 7, no. 1, 2018, doi: 10.1149/2.0121801jss.
- [21] S. -I. Yamamoto, K. Ohyama, T. Ban, and T. Nonaka, "Crystal structure dependence of red to green light emission by LaOF : Yb3+/Er3+ up-conversion phosphor," *Materials Research Express*, vol. 6, no. 3, 2019, doi: 10.1088/2053-1591/aaf35a.
- [22] Z. Abbas *et al.*, "A systematic study on optoelectronic properties of Mn4+-activated Zr-based hexafluoride red phosphors X2ZrF6 (X = K, Na, Cs): first-principles investigation and prospects for warm-white LEDs applications," *Physica Scripta*, vol. 96, 2021, doi: 10.1088/1402-4896/abc646.
- [23] X. -L. Dou, X. -Y. Kuang, X. -X. Xia, and M. Ju, "Exploration of the structural and optical properties of a red-emitting phosphor K2TiF6:Mn4+," *Chinese Physics B*, vol. 28, no. 1, 2019, doi: 10.1088/1674-1056/28/1/017107.
- [24] L. A. D. -Torres *et al.*, "Long-lasting green, yellow, and red phosphorescence of carbon dots embedded on ZnAl2O4 nanoparticles synthesized by a combustion method," *Journal of Physics D: Applied Physics*, vol. 51, no. 41, 2018, doi: 10.1088/1361-6463/aadbd.
- [25] J. Sun *et al.*, "Three Times Lifetime Improvement of Red-Emitting Organic Light-Emitting Diodes Based on Bipolar Host Material," *ECS Journal of Solid State Science and Technology*, vol. 7, no. 5, 2018, doi: 10.1149/2.0281805jss.
- [26] R. Liu and X. Wang, "Luminescent properties of a novel green phosphor CePO4-6LaPO4:Tb3+," *IOP Conference Series: Earth and Environmental Science*, vol. 267, no. 3, 2019, doi: 10.1088/1755-1315/267/3/032101.

BIOGRAPHIES OF AUTHORS

Van Liem Bui    received a Bachelor of Mathematical Analysis and master's in mathematical Optimization, Ho Chi Minh City University of Natural Sciences, VietNam. Currently, He is a lecturer at the Faculty of Fundamental Science, Industrial University of Ho Chi Minh City, Viet Nam. His research interests are mathematical physics. He can be contacted at email: buivanliem@iuh.edu.vn.



Nguyen Thi Phuong Loan    was born in Da Nang province. In 2006, She received her master degree from University of Natural Sciences. Her research interest is optoelectronics. She has worked at the Faculty of Fundamental 2, Posts and Telecommunications Institute of Technology, Ho Chi Minh City, Vietnam. She can be contacted at email: ntploan@ptithcm.edu.vn.



Hai Minh Nguyen Tran    received the B.Eng. degree in Ship Electrical and Automation Engineering and the M.Eng. degree in Control Engineering and Automation from the HCM Transport University in Ho Chi Minh City, Vietnam, in 2002 and 2017, respectively. From 2002 to 2004, he was a lecturer at Ho Chi Minh City University of Transport. From 2004 to 2009, he was a lecturer at Ho Chi Minh City University of Industrial. From 2009 to 2019, he was a Director of service and repairing workshop at Vietranstimex Holding Stock Company. Since 2019, he decided to take up a research intensive role and since a senior lecturer at Van Lang University. His research interest includes applied automation, electric SPMT, and robotics. He can be contacted at email: minh.nth@vlu.edu.vn.